Journal of
Renewable Energy Research and Applications (RERA)

Vol. 6, No. 2, 2025, 221-236 *DOI: 10.22044/rera.2025.15338.1370*

An Attempt towards Green Port Concept using Ocean Wave Energy in Chabahar Port

K. Soleimani[1], A. Gharechae[2*] and M. J. Ketabdari[1]

1. Department of Maritime Engineering, Amirkabir University of Technology, Tehran, Iran.
2. Chabahar Maritime University, Iran.

Received Date 12 November 2024; Revised Date 03 February 2025; Accepted Date 14 February 2025
**Corresponding author: a.gharechae@cmu.ac.ir (A. Gharechae)*

Abstract
This research work evaluates the feasibility of utilizing wave energy at Chabahar port as an alternative power source. The first part of the study analyzed seasonal and annual wind and wave characteristics, as well as the directional distributions of winds and waves, utilizing long-term buoy measurements. The extractable power output was determined based on the wave scatter diagram for Chabahar port and the power matrix of various existing wave power devices. The average annual wave power at this location is 4.1 kW/m. However, wave power exhibited significant variation across the autumn, winter, spring, and summer seasons, averaging 1.46, 1.48, 4.4, and 6.94 kW/m, respectively. Among the thirteen wave power concepts evaluated, the wave dragon, and the 1500 kW Pelamis demonstrated the best performance. The wave dragon is identified as the preferred wave power device for Chabahar Port, considering its power production capability, seabed compatibility, and adaptability to diverse meteorological conditions. Additionally, RETScreen Expert software was employed to conduct a cost and emissions analysis, indicating that the wave dragon and Pelamis can reduce greenhouse gas emissions by 719.7 and 351.6 tons of carbon dioxide, respectively. Consequently, the wave dragon offers the most economical power solution for Chabahar Port, with a greater reduction in greenhouse gas emissions.

Keywords: *Green Port Concept; Renewable Energy; Wave Energy; Chabahar Port; RETScreen Software.*

1. Introduction

Over the past few decades, shipping has experienced significant growth, contributing to nearly 90% of global trade. However, this rapid expansion has placed a considerable pressure on the environmental pollution control. To meet the energy demands of vessels, diesel engines rely on fossil fuels, which emit substantial pollution in port areas. Auxiliary engine exhausts represent a primary source of air pollution from berthing ships [1]. Reducing greenhouse gas emissions and other air pollutants at ports poses a major challenge for the shipping industry [2]. Port authorities can mitigate air pollution, which impacts human health and climate change, by implementing emission reduction plans and projects [3]. The management of vessel pollution in ports is typically achieved through cold ironing, the use of Liquefied Natural Gas (LNG), and the reduction of vessel speed in port areas. A shoreside electricity system provides hotel power, eliminating the need for auxiliary generators on vessels. Supplying the necessary power for cooling, heating, lighting, and air conditioning from the grid or renewable sources will decrease onboard generator operations, and offer an emission-free solution at the port, thereby reducing particulate matter (PM_{10}) and CO_2 emissions from ships [4].

To facilitate the transition from fossil fuels to sustainable energy sources, numerous green port strategies have been implemented globally in response to the urgent energy crisis, climate change, and environmental pollution. Figure 1 illustrates the top ten environmental priorities for EU ports in 2022, with air quality and energy efficiency ranking highest. The adoption of renewable energy, reduction of energy consumption, and promotion of eco-friendly mobility are integral components of energy management plans [5]. In many ports, the green port policy has been effectively executed through the implementation of environmentally sustainable strategies [6].

Figure 1. Environmental priorities for European ports

Located in southeastern Iran, near the warm waters of the Oman Sea and the Indian Ocean, Chabahar provides Afghanistan, Turkmenistan, Kazakhstan, Kyrgyzstan, and Uzbekistan with convenient access to open waters for exports (see figure 2). As a result, the port has attracted substantial investment in recent years. Given this development, the implementation of green port strategies in the region is of paramount importance.

Figure 1. The most important ports of Iran.

A number of studies have been conducted on the utilization of renewable energy in the port of Chabahar, specifically focusing on solar and wind power conversion [8-10]. Additionally, harnessing marine renewable energies including wind, wave, and tidal energies—collectively referred to as wet renewable energies—presents another viable solution [11]. Among the most prominent wet renewable energy sources, wave energy has the potential to significantly mitigate global energy demand [12].

To evaluate the nearshore wave energy and select the most suitable wave power device for Chabahar Port, a literature review was conducted on studies related to Iran's wave energy potential. Abbaspour and Rahimi (2011) performed an annual assessment of tidal and wave energies in the Persian Gulf and the Oman Sea [13]. Rashid and Hassanzadeh (2011) identified an offshore site with a depth of 1,000 meters as the optimal location for wave power in Chabahar, noting waves with $H_s = 1.2$ m and $T_p = 9.5$ s as the most energetic. They proposed a 300 kW wave energy absorber for wave energy extraction [14]. Utilizing the SWAN model, Saket and Etemad-Shahidi (2012) evaluated the wave energy potential along the Iranian coasts of the Oman Sea, recommending a region near Chabahar with an average wave power of 2.8 kW/m as the most suitable for wave power generation. Their findings indicated that the majority of annual wave power occurs at wave heights between 1-3 m and periods of 4-8 s in the SSE direction [15]. Kamranzad et al. (2013) employed the SWAN model in conjunction with ECMWF wind fields to assess wave power potential in the Persian Gulf, concluding that most wave energy can be extracted during the winter months [16]. Kamranzad et al. (2016) evaluated the wave power potential of the Oman Sea, using the SWAN model, discovering an increase in wave power from the Strait of Hormuz towards the Indian Ocean. They recommended two sites near Pasabandar and Chabahar port for harnessing wave energy, noting that summer and autumn yield the highest and lowest wave power, respectively [17]. Majidi Nezhad et al. (2018) analyzed one-year buoy data to evaluate nearshore Wave Power conversion at six sites including Chabahar, recommending the wave dragon, wave star, and Oyster for nearshore installation [18]. Kamranzad (2018) conducted a spatiotemporal analysis of wind and wave variations in the Persian Gulf, finding that both energy sources are more prevalent in winter, spring, summer, and autumn, respectively [19]. Khalifehei et al. (2018) performed a numerical analysis of the Sea Slot-cone Generator (SSG) wave energy device's performance under waves in the southern seas of Iran, concluding its suitability for use in the Gulf of Oman [20]. Khojasteh et al. (2018) reviewed state-of-the-art studies on wave and tidal energies in the Caspian Sea, Persian Gulf, and Oman Sea, including the Chabahar region, proposing heaving buoys, single point absorbers, and attenuator systems for harnessing Wave Power [21]. Pasha Zanous et al. (2019) investigated wave energy conversion at seventeen potential sites along the southern coasts and islands of Iran, focusing on manufacturing feasibility and applicability to port structures rather than power output of various devices [22].

In an effort to implement green port strategies at Chabahar port, this paper evaluates the feasibility of utilizing wave energy as a source of renewable power. An analysis of absorbed power is conducted based on the seasonal and annual wave

scatter diagrams of the area, as well as the power matrices of various wave energy converters. A list of potential wave energy converters is also included. Finally, RETScreen Expert software is employed to assess the reduction in greenhouse gas emissions resulting from the installation of wave power devices, along with a cash flow analysis of the selected devices.

2. Matrials and methods

Initially, the methods for evaluating Wave Energy at a specific location are outlined. Subsequently, the formula for estimating wave power is presented. A concise explanation of wave scatter diagrams and the procedures for determining wave power at a given location will follow. Finally, the principles of directional distribution of wind and waves are discussed.

2.1. Evaluating wave energy resource of a given location

The most common method of recording sea surface oscillations is by using small wave buoys. In addition to recording data onboard, the device transmits that data to a shore station via a telemetry system. Data collected from wave buoys is commonly used to assess the Wave Energy potential of a given location [23-26]. To obtain a representative sample of wave conditions, wave buoys typically measure the conditions for approximately 20 to 30 minutes [27]. It is necessary to conduct measurements for at least one year to demonstrate seasonal variations in sea state. Given that the wave climate differs from year to year, longer measurements are desirable. Using long-term buoy data (at least ten years) allows for an appropriate evaluation of wave power over time [28]. It is also beneficial to use long-term numerical models that span several decades to understand the interannual fluctuations in wave energy resources [27].

2.2. Wave power estimation

In general, wave motion can be described by a regular or sinusoidal wave whose height, length, and period remain constant. The following equation calculates the average energy of a regular wave per unit area under deep water conditions:

$$\mathbf{E_w} = \frac{\boldsymbol{\rho g H_s^2}}{\mathbf{16}} \quad (1)$$

where E_w represents the average wave energy per unit area ($\mathrm{J/m^2}$), ρ denotes the density of the seawater ($\mathrm{kg/m^3}$), g indicates the acceleration due to gravity ($\mathrm{m/s^2}$), and H_s refers to the significant wave height (m) [29]. To estimate the Power of a Wave per unit of wave-front width, the following equation may be employed [30]:

$$\mathbf{P_W} \approx \mathbf{0.49 H_s^2 T} \quad (2)$$

where P_W represents the power per unit of wave-front width ($\mathrm{kW/m}$), and T denotes the wave period (s).

2.3. Evaluating energy production capabilities of wave energy converters at specific locations

The efficiency of a Wave Energy converter is strongly related to the wave climate of the installation site. The most effective Wave Energy device for a given location is determined by its maximum performance within the range of prevailing significant wave heights and peak periods. The amount of Wave Power that can be generated by a wave energy converter when installed at a particular location is one of the most important factors influencing the selection of an appropriate wave energy converter. To estimate the amount of electric power generated by a given device at a specific location, a proper wave resource assessment must be conducted. An annual electricity production can be calculated by multiplying the wave resource matrix by the power matrix of the device. Wave scatter diagrams are useful tools for describing the wave resource at a given location. The diagram illustrates the occurrence of various combinations of wave height and period. This matrix should be computed under a specific methodology, and cover a significant portion of the total energy resource in order to achieve a certain level of resolution (such as the power matrix of a device).

$$\mathbf{E_0} = \sum_{\mathbf{i=1}}^{\mathbf{nT}} \sum_{\mathbf{j=1}}^{\mathbf{nH}} \mathbf{p_{ij} P_{ij}} \quad (3)$$

where p_{ij} denotes the percentage of occurrences of each sea state defined by significant wave height and energy period, and P_{ij} represents the electrical power yield provided by each wave power device for the corresponding wave. For each i and j, $E'_{0_{ij}}$ is defined by equation (4):

$$\mathbf{E'_{0_{ij}}} = \mathbf{p_{ij} P_{ij}} \quad (4)$$

2.4. Directional distribution of wind and wave

The analysis of wave buoy data is a widely utilized method for determining wave characteristics at specific locations. This study will analyze wind and wave data collected by the Chabahar buoy to assess the characteristics of wind and waves at this coastal site. The data has been provided by the Port and Maritime

Organization of Iran. Additionally, data from the Chabahar buoy has been compared with historical data from ECMWF [13], [22]. To derive seasonal and annual wave characteristics, the raw data were categorized into four classes, each corresponding to a season.

3. Different wave energy devices

The purpose of this research work is to identify the most efficient device for capturing wave energy at Chabahar port. Before evaluating various technologies, this section offers a concise overview of well-known Wave energy converters.

3.1. Point absorber

By utilizing a float with a diameter significantly smaller than the incoming wavelength, this bottom-mounted or floating device extracts wave energy from ocean waves [32]. During the interaction between the wave and the device, it undergoes heave or pitch motion, which can be harnessed as a source of shaft power, air pressure, or fluid pressure to generate energy. A shoreline or offshore installation can convert the generated power into electricity. Generally, point absorbers are most effective in offshore deep waters [33]; however, some shoreline or nearshore devices have been developed in recent years. An example of this device is illustrated in figure 3a.

3.2. Oscillating water column

In an OWC device, energy is harnessed from the wave-induced vertical motions of water within a partially submerged duct that has an open end to the sea. This vertical movement of the water column compresses, and decompresses the air within the chamber, enabling the generation of turbine power. By creating a narrower air channel before the turbine, the air current within the chamber can be accelerated, thereby enhancing the device's efficiency [34]. However, friction with the seafloor diminishes the energy generated by waves at coastal locations. An OWC is illustrated in figure 3b.

3.3. Attenuator devices

A wave attenuator comprises a stationary component and a moving component aligned perpendicularly to the direction of the wave. By utilizing the relative motions of two or more floating segments, double-action pumps can be derived for the extraction of wave energy [29]. Pelamis and WaveStar are the most prominent devices of this type. A schematic representation of the WaveStar device is presented in figure 3c.

3.4. Overtopping Devices

Considering that overtopping devices consist of stationary components; they are less vulnerable to wave effects. Consequently, they are suitable for use in all weather conditions, whether nearshore or offshore. These devices capture seawater from incident waves and store it above the mean sea level in a reservoir. After passing through a conventional low-head turbine, the water is released back into the sea to generate electricity. Overtopping devices are most commonly utilized near coastal deep waters with small tidal amplitudes and rocky coastlines. An example of this type of wave energy converter is the Wave Dragon, as shown in figure 3d.

3.5. Submerged pressure differential converters

Water surface oscillations create a pressure differential on the seabed. Most submerged pressure differential devices are deployed nearshore on the seabed and utilize this differential pressure to pump fluid through a system for electricity generation. A schematic representation of the submerged pressure differential device is presented in figure 3e.

3.6. Hybrid concepts

To enhance absorbed power, a combination of wave power devices or their integration into other structures has been proposed. For instance, hybrid wind-wave devices based on the WaveStar concept have been suggested in [35-37]. Additionally, studies have examined combined Wave Power devices with other structures as platforms [38, ships [39] and fish cages [40, 41]. These concepts have not been examined in the current research work.

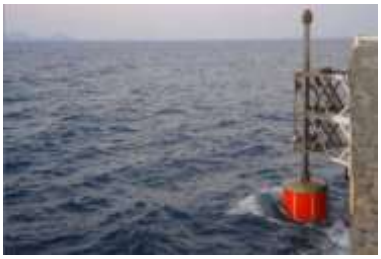

a)

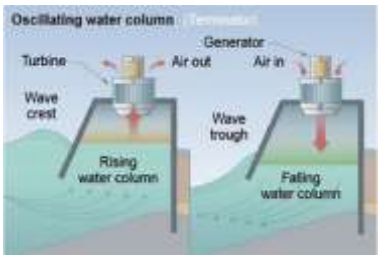

b)

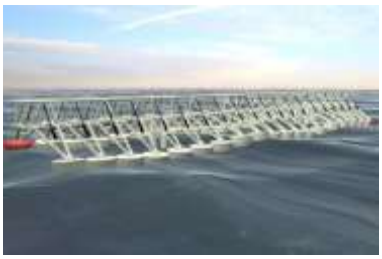

c)

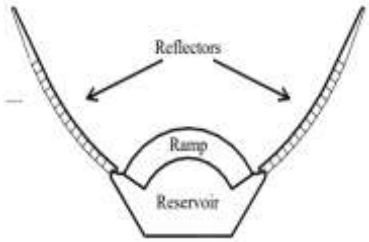

d)

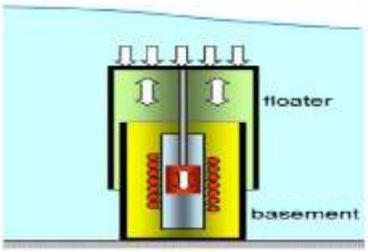

e)

Figure 3. Concepts proposed for wave energy conversion: a) point absorber; b) oscillating water column; c) attenuator device (Wave Star); d) overtopping Wave Energy device; and e) submerged pressure differential converter [23, 24, 25].

4. Effect of shore type on selection of a wave energy device

The type of shoreline influences the selection of the most appropriate Wave Energy converter for a specific location. Onshore Wave Energy converters necessitate either rocky cliffs, as exemplified by LIMPET on Islay Island, or rocky gullies such as those found on Pico Island, for the construction of the converter structure [42]. As a coastal defense mechanism, overtopping Wave Energy devices, like the one proposed by Buccino et al. (2015) are less likely to require extensive construction efforts on rocky shorelines [43]. However, certain devices, such as the Terobuoy, a point absorber, may be susceptible to damage from the harsh conditions of rocky shores, as well as from sediments and flotsam that may become entrained in the device [44].

5. Effect of WECs on marine life

The main consequences of implementing Wave Energy Converters (WECs) on marine life, as outlined in the paper, include:

1. Collision risk: Fish may encounter the moving parts of WECs, potentially leading to injury or mortality. However, the risk is generally considered low, compared to the traditional hydropower turbines.
2. Underwater noise: Operational noise from WECs may affect fish behavior and communication. Most noise falls within the hearing range of many fish species but is typically at lower volumes than other marine noise sources, suggesting minimal harm.
3. ElectroMagnetic Fields (EMFs): EMFs generated by cables associated with WECs can affect sensitive fish species. However, studies indicate that the levels from WECs are unlikely to have significant impacts on marine life.
4. Changes in habitat: The installation of WECs can disturb benthic habitats, and alter the structure of local ecosystems. These devices may also attract fish, acting as artificial reefs.
5. Fish aggregation: WECs might inadvertently function as Fish Aggregating Devices (FADs), attracting certain species and potentially altering local fish populations.
6. Displacement: There is a potential for fish to be displaced from their natural habitats due to the presence of WEC arrays, although this effect remains under-researched.
7. Cumulative Effects: The interaction of WECs with other anthropogenic stressors such as climate change and coastal development, may compound the impacts on fish populations and ecosystems.

Overall, while there are potential risks to marine life from WECs, the extent of these impacts varies and requires further research to fully understand [45].

6. Studied area

The port of Chabahar (60.65 E and 25.267 N) is situated in southeastern Iran, along the northern coast of the Oman Sea. This region is characterized by a moderate tropical climate, with summer monsoon winds from the Indian Ocean making Chabahar the coolest area in southern Iran during the summer months. These monsoons also generate significant wave activity. The average temperature in this region is 26.5 $^{\circ}$C [46]. It is projected that by 2060, 95% of the energy required by the city of Chabahar will be utilized for cooling purposes, indicating that a substantial portion of the city's energy demands will occur during the summer and spring months. Chabahar, located on the Indian Ocean, experiences a dynamic wave climate, with previous studies

indicating that waves primarily originate from the southeast [15].

There are two major ports in Chabahar: Shahid Beheshti and Shahid Kalantari. The locations of these ports are depicted in figure 4. The coastal classification of the Chabahar area is shown in figure 5a, indicating that the port is situated in a region with rocky seabeds [48]. Figure 5b illustrates a similar shoreline at the port's location. The annual energy consumption of Shahid Beheshti Port is 9,992 MWh [49].

Figure 4. An aerial photo of the Chabahar port.

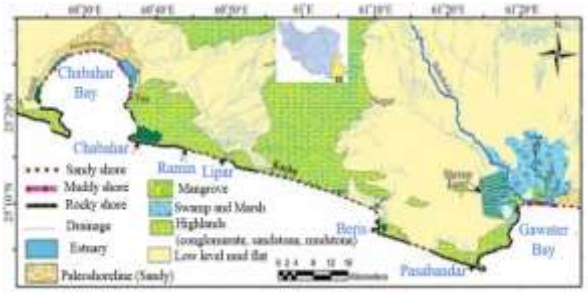

a)

b)

Figure 5. a) GIS-based map showing the coastal classification of the area [48] and b) an illustration of the shoreline type at Chabahar port.

Figure 6 illustrates the bathymetry map of the Chabahar area, along with the location of the Chabahar wave buoy. The bathymetry map indicates that the water depth near Chabahar Port is less than 50 meters.

7. Results and discussion

7.1. Wind and wave characteristics

In this study, buoy measurements from 2010 to 2020 were utilized to analyze the wind and wave characteristics at Chabahar port. The data were provided by the Iranian ports and maritime organization.

Table 1 presents seasonal and annual values for significant wave height (H_s), peak wave period (T_p), Mean Wave Power (MWP), Mean Wave Direction (MWD), Wind Speed (W_s), and Wind Direction (WD). The spring and summer seasons exhibit elevated significant wave heights, peak periods, and power values. The average seasonal significant wave height at this station is 0.56 meters in winter and 1.33 meters in summer.

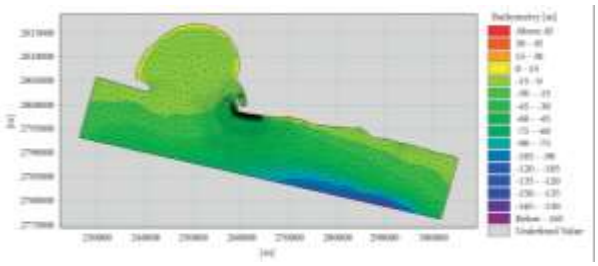

a)

b)

Figure 6. a) Bathymetry map of the area [50] and b) The location of the Chabahar Wave buoy.

During the summer season, the maximum seasonal mean wave height and peak period are 1.34 m and 9.14 s, respectively. In contrast, autumn exhibits the lowest average significant wave height, with a mean value of 0.56 m. Additionally, wave power fluctuates significantly across seasons. For instance, the available power in autumn and winter is approximately 1.46 and 1.48 kW/m, while in spring and summer, it is approximately 4.4 and 6.95 kW/m. The mean annual wave power is about 4.1 kW/m.

Furthermore, the data indicates that mean wind speeds are higher in the winter season compared to other seasons.

Table 1. Wave and wind characteristics of Chabahar port in different seasons.

	Autumn	Winter	Spring	Summer	Annual
H_s (m)	0.563	0.635	0.924	1.332	0.877
T_p (s)	7.651	6.142	8.497	9.149	7.866
MWP (kW/m)	1.459	1.482	4.378	6.946	4.071
MWD	182.1	197.7	183.5	170.0	183.4
W_s (m/s)	3.250	4.165	3.542	4.079	3.784
WD	192.3	200.1	202.	159.6	188.2

In figure 7, the seasonal variations in wind direction are evident in the directional distribution of wind. As previously noted, the area is significantly influenced by monsoon winds from various directions. Chabahar port experiences monsoon winds from the Indian Ocean during the summer months, resulting in a predominant wind direction shift to the southeast. Furthermore, the figure illustrates that spring exhibits the highest maximum wind speed, followed by autumn. Table 1 indicates that the mean wind speed in summer and winter exceeds that of spring and autumn. The annual wind rose for Chabahar port, presented in figure 8, demonstrates that the majority of winds are below 5.5 m/s, with the prevailing wind direction oriented from southeast to southwest.

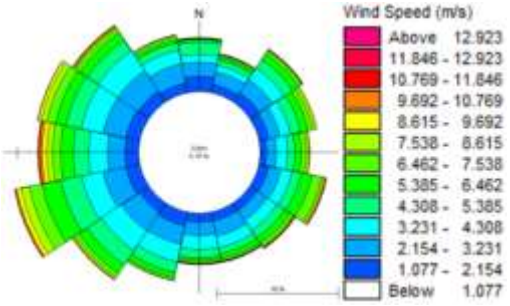

Winter Wind Rose

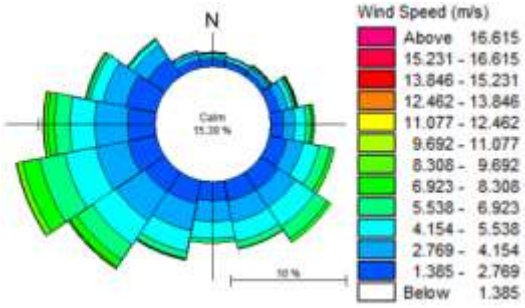

Spring Wind Rose

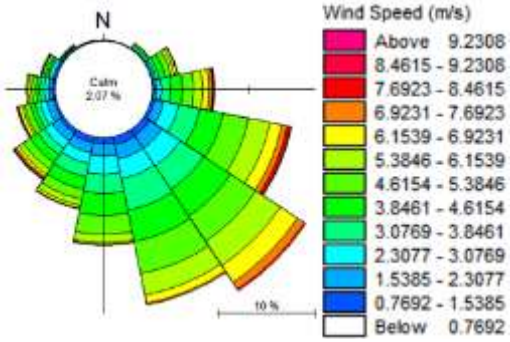

Summer Wind Rose

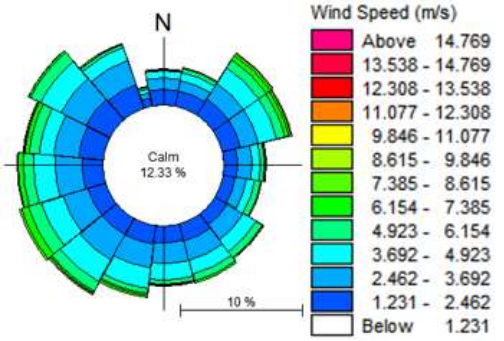

Autumn Wind Rose

Figure 7. Seasonal wind roses at Chabahar port.

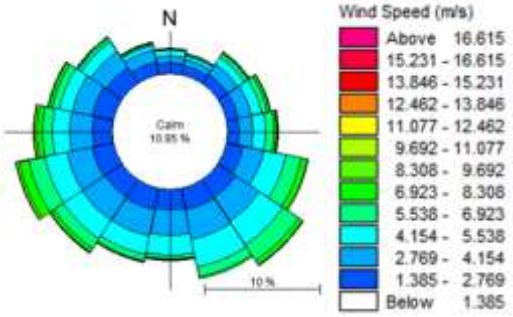

Figure 8. Annual wind rose at Chabahar port.

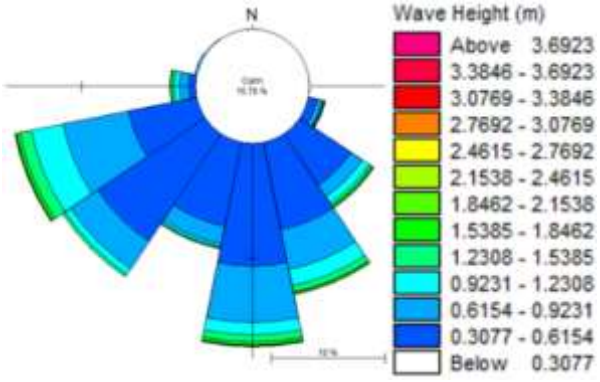

Winter Wave Rose

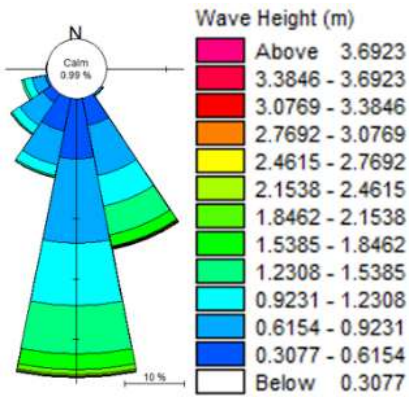

Spring Wave Rose

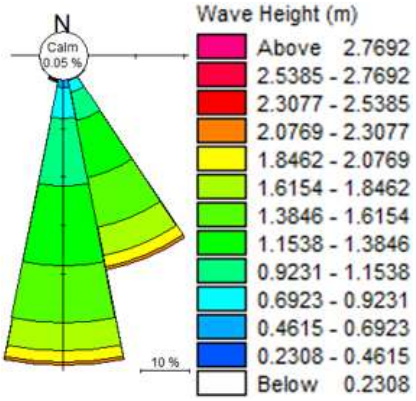

Summer Wave Rose

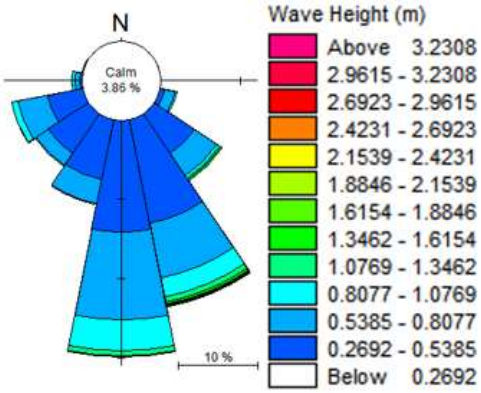

Autumn Wave Rose

Figure 9. Seasonal wave roses at Chabahar port.

According to the seasonal wave roses illustrated in figure 9, the direction of the dominant wave is influenced by the season. In spring, summer, and autumn, the predominant Wave Direction is south to southeast, while in winter, waves originate from the south to southwest. Figure 10 clearly indicates that most waves do not exceed 1.5 meters in height. This figure further demonstrates that the predominant wave direction on an annual basis is south to southeast, aligning with previous studies [15].

As illustrated in figure 1, wave power extraction from the sea at Chabahar port is greater during the spring and summer months when cooling energy is in demand. Conversely, Wave Power is at its lowest during the autumn season. There exists a distinction between the seasonal distribution of Wave Power and wave height, as Wave Power is influenced by both wave height and wave period. Nonetheless, this figure demonstrates that wave power is predominantly concentrated in the south-southeast direction. The annual wave power rose is depicted in figure 12, further confirming this concentration. According to table 1, the mean annual wave power in the area is approximately 4.1 kW/m, which is comparable to other regions worldwide, such as the southeastern USA at 15 kW/m [51], the southeastern Black Sea at 7 kW/m [52], and the Egyptian coast of the Mediterranean Sea at 4 kW/m [53].

An illustration of the wave scatter diagram for Chabahar port is presented in figure 13. The wave height and period intervals in this matrix have been established using power matrices for certain devices (D1-D8) previously introduced by Babarit et al. (2012) [54].

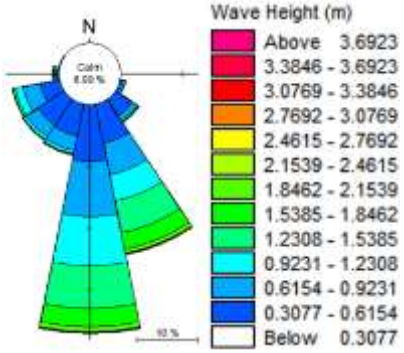

Figure 10. Annual wave rose at Chabahar port.

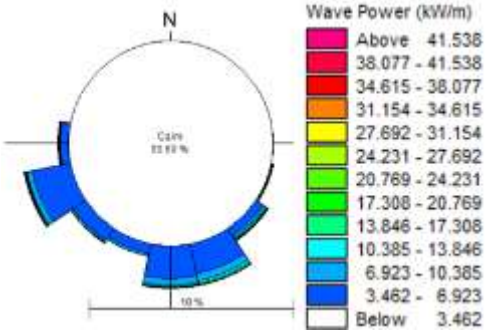

Winter Wave Power

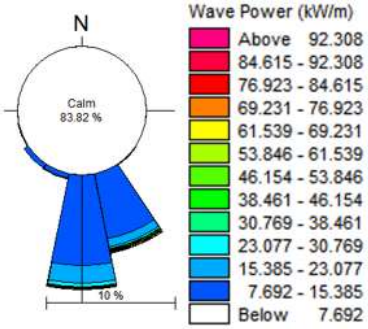

Spring Wave Power

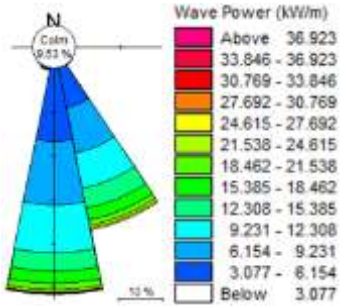

Summer Wave Power

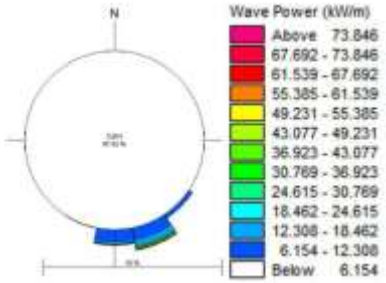

Autumn Wave Power

Figure 11. Seasonal wave power rose at Chabahar port.

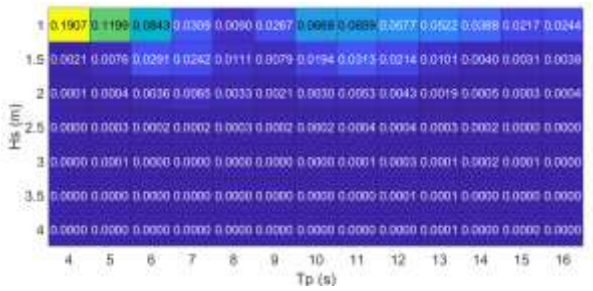

Figure 13. Wave scatter diagram for Chabahar port.

7.2. Selection of suitable technology for wave energy harvesting in Chabahar port

The power matrices of various devices including the small bottom-mounted heaving buoy (D1), submerged bottom-mounted heaving buoy (D2), floating two-body heaving converter (D3), arrays of bottom-mounted heaving buoys (D4), arrays of floating heaving buoys (D5), bottom-fixed oscillating flap (D6), floating three-body oscillating flap device (D7), floating oscillating water column (D8), 750 kW Pelamis (D9), 1500 kW Pelamis (D10), 750 kW single point absorber (D11), Wave Dragon (D12) and WaveStar (D13) are utilized to calculate the performance of each device at Chabahar port.

The small bottom-referenced heaving buoy has a diameter of 3.0 m, a draft of 0.63 m, and a displacement of 2.83 cubic meters. Its mass is 1.0 ton, and its stroke length is 1.8 m. The device can be installed in water depths ranging from 40 to 100 m [54].

The bottom-referenced submerged heave buoy has a diameter of 7.0 m, a height of 5.0 m, and a displacement of 148 cubic meters. Its mass is 35 tons, its stroke length is 6.0 m, and it can be installed in a water depth of 20.0 m [54].

The floating two-body heaving converter features a torus diameter of 20.0 m, a torus draft of 2.0 m, and a float draft of 50.0 m, with a displacement of 4960 cubic meters. The mass of the torus is 278 tons, while the mass of the float is 4680 tons, and its stroke length is 6.0 m. This device is designed for deep water applications [54].

The bottom-fixed heave-buoy array consists of 20 floats, each with a diameter and height of 5.0 meters. The float displacement and mass are 25.5 cubic meters and 35 tons, respectively. The dimensions and mass of the structure are 70 meters in length, 17.0 meters in width, and 900 tons. The device is intended for installation in a water depth of 13.0 meters [54].

The floating heave-buoy array is a multibody floating Wave Energy Converter (WEC) composed of ten floats. Each float has a diameter of 8.0 meters, a draft of 13.4 meters, and a displacement of 406 cubic meters. The mass of each float is 364 metric tons. The overall length of the structure is 132 meters, its width is 18 meters, and the total mass of the structure is 467 metric tons [54.

The bottom-fixed oscillating flap is a straightforward pitching flap that oscillates about a fixed axis near the seabed, making it suitable for shallow and intermediate waters. The structure has a width of 26.0 meters, a draft of 9.0 meters, and dimensions of 2.0 meters in width and 4.0 meters in thickness. Additionally, the mass and displacement of the device are 150 tons and 442 m^3, respectively [54].

The floating three-body oscillating flap comprises four hinged flaps connected to a single floating structure. The flap has a width of 9.5 meters, a draft of 8.5 meters, and a displacement of 185 cubic meters. The structure measures 25 meters in length and width, with a draft of 12.0 meters and a displacement of 673 cubic meters [54].

The floating oscillating water column under consideration is a Backward Bent Duct Buoy (BBDB). This device features a single air chamber and is capable of movement in six degrees of freedom. Its dimensions are as follows: length of 50 meters, width of 24 meters, and draft of 13 meters [54].

The main dimensions of the wave dragon device considered in this study are shown in the figure 14 [55].

PELAMIS P1 (750 kW) was 120 meters long, 3.5 meters in diameter, and comprised four tube sections. PELAMIS P2 (1.5 MW) measured 180

meters in length, four meters in diameter, and consisted of five tube sections [56].

The hypothetical 750 kW single point absorber has a natural period of 11 seconds, a damping coefficient of 0.06, an efficiency of 80%, a radius of 6 meters, and a stroke of 3 meters [57].

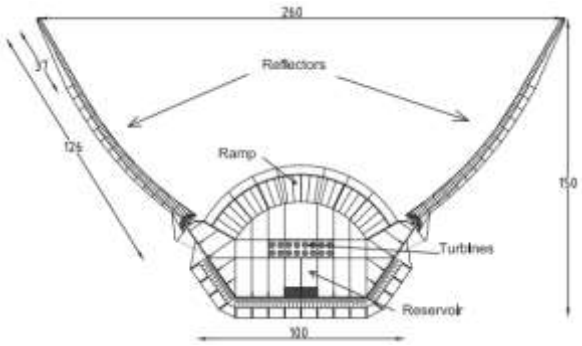

Figure 14. Main structural elements of the wave dragon.

The Wavestar WEC considered in this study is equipped with 20 floats, each float having a diameter of 6 m. The individual float is mounted on a 12 m long steel arm, which is hinged to the main tube. Ten arms are placed on each side of the tube [58].

A wave scatter diagram should be provided, reflecting the same wave height and period intervals discussed earlier in the paper. Equations 3 and 4 are employed to determine the absorbed power. For instance, the power matrix of D6 is illustrated in figure 15, with its corresponding E_0' matrix for annual power production presented in figure 16. By summing the values in figure 16, we can ascertain the potential E_0 that can be harnessed with D6. Similar calculations should be conducted for the other devices to determine E_0' and E_0.The power matrices for D1-D8, D9-D11 and D12-D13 can be found in references [14], [31], [54].

There is, however, a seasonal variation in the amount of power generated by all devices, with more power being generated during the summer months. This is illustrated in figure 17. Wavestar and heaving buoy arrays exhibit less As shown in figure 18, in summer, Pelamis and Wave Dragon are capable of generating up to 1050 kW.

Figures 17-18 illustrate the exploitable power of each device. It is evident that, on an annual scale, the Wave Dragon (683.9 kW), 1500 kW Pelamis (494.6 kW), 750 kW single point absorber (238.6 kW), arrays of heaving buoys (133.9 kW), and Wavestar (117.3 kW) can generate more power at Chabahar port. The small bottom-mounted heaving buoy, generating only 1.253 kW, is the least efficient device. At Chabahar port, the Wave Dragon's exploitable power is comparable to that of other global locations. In Romania's nearshore and Brittany, two of the most energetic regions worldwide, the Wave Dragon achieved annual mean powers of 391.79 kW and 1495 kW, respectively [59, 60]. Given that the seabed at Chabahar port consists of rocky material, the use of overtopping devices such as the Wave Dragon may be appropriate.

Based on the bathymetric map of Chabahar port, all floating converters can be moored at depths of approximately 30 to 45 meters. However, there is a seasonal variation in power generation, with increased output during the summer months, as illustrated in figure 17. Wavestar and heaving buoy arrays demonstrate less seasonal variation. As shown in figure 18, Pelamis and Wave Dragon can generate up to 1,050 kW in summer.

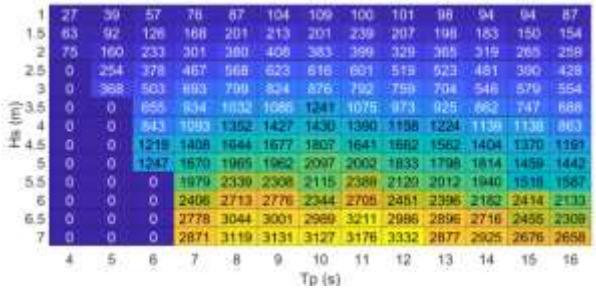

Figure 15. Power matrix for [48]

The final selection of the device and the installation location of a wave power device in a coastal region should consider additional parameters including installation and operational expenses, as well as potential environmental consequences that require further research and are beyond the scope of this paper.

By applying various limitations including a minimum distance of 1,000 meters from protected areas, 500 meters from undersea oil and gas pipelines, and 500 meters from shipping lanes, Einali et al. (2022) identified the optimal locations for establishing a wave power plant using ArcGIS 10.3 [61]. These locations are illustrated in figure 18.

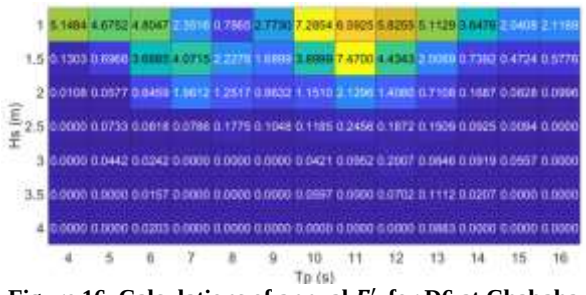

Figure 16. Calculations of annual E_0' for D6 at Chabahar port.

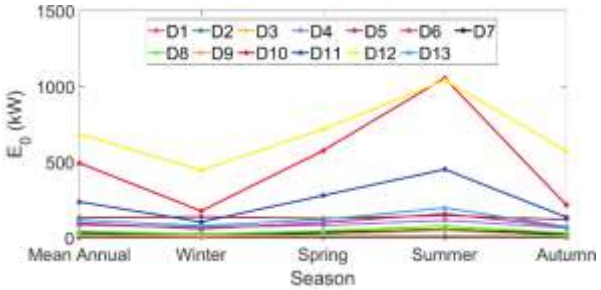

Figure 17. Variations in the seasonal energy production of different devices in the Chabahar port.

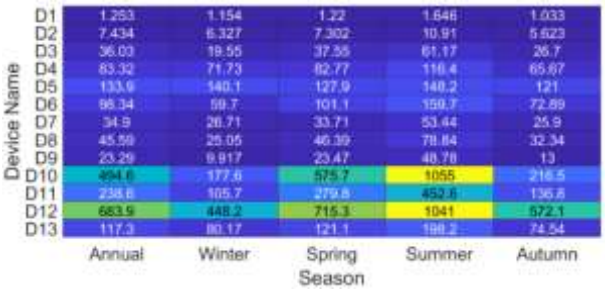

Figure 18. Calculation of extractable power (in kW) for various devices at Chabahar port based on available power matrices.

Figure 19. Locations proposed for Wave Power device installation.

7.3. Cost and Emission calculations

Based on the calculations of exploitable power presented in the previous section, Wave Dragon and Pelamis, which exhibit the highest exploitable power, have been selected for emissions and cost calculations. All emission and cost analyses in this section are conducted using RETScreen Expert software [62]. The assumptions utilized for the cost analysis are detailed in table 2.

Table 2. Financial parameters used in the analysis.

Financial parameter	Value	Unit
Inflation rate	2.0	%
Fuel escalation rate	2.0	%
Debt ration	70.0	%
Discount rate	9.0	%
Debt term	15	Years
Debt interest rate	7	%
System life-time	25	Years
Reinvestment rate	9	%

7.4. Costs and emissions associated with Wave Dragon

The Wave Dragon device costs approximately $2,400 per kW, with maintenance costs ranging from 3% to 6% annually. It has a capacity factor of 0.34 [63]. With a capacity of 683.9 kW, the Wave Dragon device can generate 1,498 MWh of electricity, sufficient to meet 15% of the port's energy requirements. The primary source of electricity in Iran is natural gas, which emits 0.481 tons of CO_2/MWh and incurs a transmission and distribution (T&D) loss of 7.0%. The RETScreen Expert software calculated the GreenHouse Gas (GHG) emissions in the base case to be 773.9 tons of carbon dioxide (tCO_2), compared to 54.2 tCO_2 for the Wave Dragon device. Based on the net annual reduction in GHG emissions achieved by the Wave Dragon device in Chabahar, equivalent cases are presented in table 3.

A simulation of the financial parameters for an investment in Wave Dragon at Chabahar port, along with the projections outlined in table 3, yields an Internal Rate of Return (IRR) of 8.0 percent and an equity payback period of 16.4 years. The benefit-to-cost ratio of the investment is 0.85. Annual and cumulative cash flows are presented in figure 19, which indicates that the cumulative cash flow reaches $1,588,000 by the end of the 25th year.

Table 3. Equivalent cases substitute for Wave Dragon power plant based on net annual GHG emissions reduction in Chabahar.

Equivalent cases	Value
Reduction in CO_2 gross annual	719.7 tCO_2
Barrels of crude oil not consumed	1673.8
Cars and light trucks not used	131.8
liters of gasoline not consumed	309244.4
Acres of forest absorbing carbon	163.6
Hectares of forest absorbing carbon	66.2
Tonnes of waste recycled	248.2

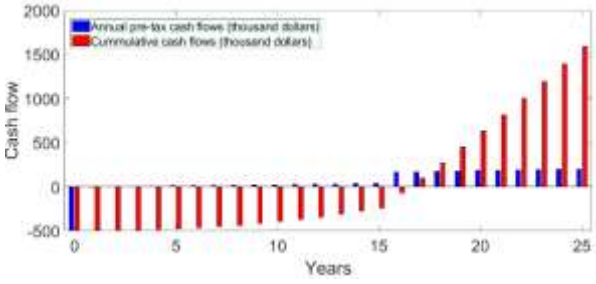

Figure 20. RETScreen Expert software cashflow graph for Wave Dragon in Chabahar port.

The unit cost of $3,333.00 per kW is required for a Pelamis device, which incurs maintenance costs

ranging from 3% to 6% annually. This device has a capacity factor of 0.4 [63]. A Pelamis wave converter can generate 732 MWh of electricity with a capacity of 463.9 kW, which meets only 7.2% of the port's energy requirements. According to an analysis conducted using RETScreen Expert software, the baseline GreenHouse Gas (GHG) emissions are 378 tCO_2, while the Pelamis device emits only 26.5 tCO_2. This results in a reduction of 351.6 tCO_2 in gross annual GHG emissions. Table 5 presents equivalent cases based on the net reduction in GHG emissions achieved by the Pelamis device in Chabahar.

According to the simulation of financial parameters for an investment in Pelamis at Chabahar port, the Internal Rate of Return (IRR) is projected to be 3.0%, with a payback period of 18.1 years. The benefits-to-cost ratio for this investment is 0.1. The cumulative cash flow over time for this investment is illustrated in figure 20, indicating a cumulative cash flow of $538,000 by the end of the 25th year.

Table 4. Equivalent cases substitute for Pelamis wave power plant based on net annual GHG emissions reduction in Chabahar.

Equivalent cases	Value
Reduction in CO_2 gross annual	351.6 tCO_2
Barrels of crude oil not consumed	817.6
Cars and light trucks not used	64.4
liters of gasoline not consumed	151063.6
Acres of forest absorbing carbon	79.9
Hectares of forest absorbing carbon	32.3
Tonnes of waste recycled	121.2

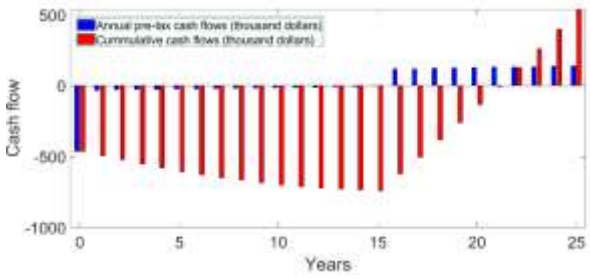

Figure 21. RETScreen Expert software cashflow graph for Pelamis in Chabahar port.

8. Conclusion

The concept of a green port strategy is an emerging field aimed at reducing the carbon footprint of ports through the utilization of various technologies. One potential solution is to supply power to ships berthed in the port using ocean renewable energy sources such as wave energy. Nearshore wave energy extraction presents an effective alternative for energy supply in ports. To evaluate the oceanographic characteristics of a specific location, long-term buoy data is typically employed. Utilizing 10 years of wave data from the Chabahar buoy, wind, wave, and wave power roses were generated for both seasonal and annual time periods, allowing for the determination of mean wind and wave characteristics. To assess the potential wave power that can be extracted by each device, we analyzed the wave scatter diagram of Chabahar Port alongside the power matrices of various devices. Based on this analysis, the following conclusions can be drawn:

- There is variability in the direction of the dominant wind in this region throughout the year. During the summer, monsoon winds predominantly blow from the southeast. Wind speeds are higher in the summer and winter seasons, with the majority of winds recorded below 5.5 m/s, and the prevailing wind direction is from southeast to southwest.
- The prevailing wave direction during spring, summer, and autumn is SSE, while in winter, it shifts to S to SW. Spring and summer are characterized by the most energetic waves; however, severe storms result in greater maximum wave heights during winter and spring. Annually, the predominant wave direction remains SSE. Additionally, wave power is more readily harnessed in spring and summer when energy demand increases due to higher temperatures. Generally, wave heights do not exceed 1.5 meters, with summer exhibiting more energetic waves. Nevertheless, spring holds the highest available wave power.
- The analysis of the mean values indicates that the maximum seasonal mean wave height and peak period are 1.34 m and 9.14 s, respectively, occurring during the summer season. The lowest mean wave height, with a value of 0.56 m, is observed in the autumn season. Additionally, there is significant variability in the available wave power in the area. For instance, the autumn and winter seasons exhibit approximately 1.5 kW/m, while the available power in spring and summer is 4.4 kW/m and 6.95 kW/m, respectively. The mean annual wave power is approximately 4.1 kW/m.
- In this study, the extractable power of 13 devices was assessed using the wave scatter diagram of the Chabahar wave, and the available power matrices of these wave energy converters. Based on the values of energy production values (E_0) of various devices, the Wave Dragon (with 683.9 kW), the 1500 kW Pelamis (with 464 kW), and the 750 kW single

point absorber (with 238.6 kW), along with arrays of heaving buoys (with 133.9 kW) and Wavestar (with 117.3 kW), are identified as the most suitable wave power devices for Chabahar Port. Given the rocky seabed at Chabahar Port, overtopping devices such as the Wave Dragon are preferred.

- It was observed that the power generated by each device varies by season, with summer and spring yielding the highest outputs. The utilization of wave power devices, particularly Wave Dragon and Pelamis, which exhibit superior power generation capabilities during these seasons, presents a viable option for supplying electricity during peak summer days when consumption is elevated. The seasonal analysis indicated that Pelamis and Wave Dragon can provide up to 1,050 kW during the summer season.
- The Wave Dragon has been identified as the most effective wave power conversion device at Chabahar port, based on several criteria including its power production capacity, seabed type, and performance under varying meteorological conditions.
- According to an analysis conducted using RETScreen Expert software, the installation of the Wave Dragon device resulted in a reduction of 719 tCO2 in greenhouse gas emissions. The Internal Rate of Return for this project was determined to be 8.0%, with an equity payback period of 16.4 years. The benefit-to-cost ratio for this investment was 0.85. By the end of the 25th year, the cumulative cash flows amounted to $1,588,000.

9. Data Availability Statement

The data supporting the findings of this study are available from the corresponding author upon reasonable request.

10. Disclosure Statement

The authors affirm that there are no relevant financial or non-financial competing interests to disclose.

11. References

[1] Sadek, I. & Elgohary, M. (2020). Assessment of renewable energy supply for green ports with a case study. Environmental Science and Pollution Research, vol. 27, no. 5. doi: 10.1007/s11356-019-07150-2.

[2] Sornn-Friese, H., Poulsen, R. T., Nowinska, A. U. & de Langen, P. (2021). What drives ports around the world to adopt air emissions abatement measures Transportation Research Part D: Transport and Environment, vol. 90. doi: 10.1016/j.trd.2020.102644.

[3] Cammin, P., Yu, J., Heilig, L. & Voß, S. (2020). Monitoring of air emissions in maritime ports. Transportation Research Part D: Transport and Environment, vol. 87. doi: 10.1016/j.trd.2020.102479.

[4] Kotrikla, A. M., Lilas, T. & Nikitakos, N. (2017). Abatement of air pollution at an Aegean island port utilizing shore-side electricity and renewable energy. Marine Policy, vol. 75. doi: 10.1016/j.marpol.2016.01.026.

[5] Bjerkan, K. Y. & Seter, H. (2019). Reviewing tools and technologies for sustainable ports: Does research enable decision making in ports? Transportation Research Part D: Transport and Environment, vol. 72. doi: 10.1016/j.trd.2019.05.003.

[6] Tsai, Y. T., Liang, C. J., Huang, K. H., Hung, K. H., Jheng, C. W. & Liang, J. J. (2018). Self-management of greenhouse gas and air pollutant emissions in Taichung Port, Taiwan. Transportation Research Part D: Transport and Environment, vol. 63. doi: 10.1016/j.trd.2018.07.001.

[7] The EcoPorts website (2022). Top 10 Environmental Priorities of Ports 2022 - EcoPorts | ESPO. Available: https://www.ecoports.com/publications/top-10-environmental-priorities-of-ports-2022

[8] Mohammadi, K., Mostafaeipour, A. & Sabzpooshani, M. (2014). Assessment of solar and wind energy potentials for three free economic and industrial zones of Iran. Energy, vol. 67. doi: 10.1016/j.energy.2014.02.024.

[9] Alavi, O., Mostafaeipour, A., Sedaghat, A. & Qolipour, M. (2017). Feasibility of a Wind-Hydrogen Energy System Based on Wind Characteristics for Chabahar, Iran. Energy Harvesting Systems, vol. 4, no. 4. doi: 10.1515/ehs-2017-0003.

[10] Rezaei, M., Mostafaeipour, A., Jafari, N., Naghdi-Khozani, N. & Moftakharzadeh, A. (2020). Wind and solar energy utilization for seawater desalination and hydrogen production in the coastal areas of southern Iran. Journal of Engineering Design and Technology, vol. 18, no. 6. doi: 10.1108/JEDT-06-2019-0154.

[11] Frid, C., et al. (2012). The environmental interactions of tidal and wave energy generation devices. doi: 10.1016/j.eiar.2011.06.002.

[12] Garavelli, L., Freeman, M. C., Tugade, L. G., Greene, D. & McNally, J. (2022). A feasibility assessment for co-locating and powering offshore aquaculture with wave energy in the United States. Ocean & Coastal Management, vol. 225, p. 106242. doi: 10.1016/J.OCECOAMAN.2022.106242.

[13] Abbaspour, M. & Rahimi, R. (2011). Iran atlas of offshore renewable energies. Renewable Energy, vol. 36, no. 1. doi: 10.1016/j.renene.2010.06.051.

[14] Rashid, A. & Hasanzadeh, S. (2011). Status and potentials of offshore wave energy resources in Chabahar area (NW Oman Sea). doi: 10.1016/j.rser.2011.06.015.

[15] Saket, A. & Etemad-Shahidi, A. (2012). Wave energy potential along the northern coasts of the Gulf of Oman, Iran. Renewable Energy, vol. 40, no. 1. doi: 10.1016/j.renene.2011.09.024.

[16] Kamranzad, B., Etemad-Shahidi, A. & Chegini, V. (2013). Assessment of wave energy variation in the Persian Gulf. Ocean Engineering, vol. 70. doi: 10.1016/j.oceaneng.2013.05.027.

[17] Kamranzad, B., Chegini, V. & Etemad-Shahidi, A. (2016). Temporal-spatial variation of wave energy and nearshore hotspots in the Gulf of Oman based on locally generated wind waves. Renewable Energy, vol. 94. doi: 10.1016/j.renene.2016.03.084.

[18] Nezhad, M. M., Groppi, D. & Piras, G. (2018). Nearshore wave energy assessment of Iranian coastlines. Proceedings of the World Congress on New Technologies. doi: 10.11159/icepr18.180.

[19] Kamranzad, B. (2018). Persian Gulf zone classification based on the wind and wave climate variability. Ocean Engineering, vol. 169. doi: 10.1016/j.oceaneng.2018.09.020.

[20] Khalifehei, K., Azizyan, G. & Gualtieri, C. (2018). Analyzing the performance of wave-energy generator systems (SSG) for the Southern Coasts of Iran, in the Persian Gulf and Oman Sea. Energies, vol. 11, no. 11. doi: 10.3390/en11113209.

[21] Khojasteh, D., Khojasteh, D., Kamali, R., Beyene, A. & Iglesias, G. (2018). Assessment of renewable energy resources in Iran; with a focus on wave and tidal energy. doi: 10.1016/j.rser.2017.06.110.

[22] Zanous, S. P., Shafaghat, R., Alamian, R., Shadloo, M. S. & Khosravi, M. (2019). Feasibility study of wave energy harvesting along the southern coast and islands of Iran. Renewable Energy, vol. 135. doi: 10.1016/j.renene.2018.12.027.

[23] Lenee-Bluhm, P., Paasch, R. & Özkan-Haller, H. T. (2011). Characterizing the wave energy resource of the US Pacific Northwest. Renewable Energy, vol. 36, no. 8. doi: 10.1016/j.renene.2011.01.016.

[24] Aoun, N. S., Harajli, H. A., & Queffeulou, P. (2013). Preliminary appraisal of wave power prospects in Lebanon. Renewable Energy, vol. 53. doi: 10.1016/j.renene.2012.11.008.

[25] Kasiulis, E., Punys, P., & Kofoed, J. P. (2015). Assessment of theoretical near-shore wave power potential along the Lithuanian coast of the Baltic Sea. Renewable and Sustainable Energy Reviews. doi: 10.1016/j.rser.2014.08.044.

[26] Sulukan, E. (2018). Wave energy potential assessment for Riva and Foça, Turkey. Journal of Polytechnics. doi: 10.2339/politeknik.385825.

[27] Alcorn, R. (2014). Wave energy. In: Future Energy: Improved, Sustainable and Clean Options for our Planet, pp. 357–382. doi: 10.1016/B978-0-08-099424-6.00017-X.

[28] Kasiulis, E., Kofoed, J. P., Povilaitis, A., & Radzevičius, A. (2017). Spatial distribution of the Baltic Sea near-shore wave power potential along the coast of Klaipėda, Lithuania. Energies, vol. 10, no. 12. doi: 10.3390/en10122170.

[29] Soleimani, K., Ketabdari, M. J., & Khorasani, F. (2015). Feasibility study on tidal and wave energy conversion in Iranian seas. Sustainable Energy Technologies and Assessments, vol. 11. doi: 10.1016/j.seta.2015.03.006.

[30] Zabihian, F., & Fung, A. S. (2011). Review of marine renewable energies: Case study of Iran. Renewable and Sustainable Energy Reviews, vol. 15, no. 5, pp. 2461–2474. doi: 10.1016/J.RSER.2011.02.006.

[31] Kamranzad, B., & Hadadpour, S. (2020). A multi-criteria approach for selection of wave energy converter/location. Energy, vol. 204. doi: 10.1016/j.energy.2020.117924.

[32] Soleimani, K., Ketabdari, M. J., & Gharechae, A. (2023). Smoothed particle hydrodynamics study of a heaving point absorber in various waves using wave tank and calm-water models. Physics of Fluids, vol. 35, no. 3. doi: 10.1063/5.0142249.

[33] Soleimani, K., & Ketabdari, M. J. (2022). Performance analysis of a tuned point absorber using SPH calm water and wave tank simulations. Journal of Ocean Engineering and Science. doi: 10.1016/j.joes.2022.03.010.

[34] Soleimani, K., Ketabdari, M. J., & Bingham, H. B. (2022). WCSPH simulation of the forced response of an attenuator oscillating water column wave energy converter. European Journal of Mechanics - B/Fluids, vol. 95, pp. 38–51. doi: 10.1016/J.EUROMECHFLU.2022.04.003.

[35] Ghafari, H. R., Neisi, A., Ghassemi, H., & Iranmanesh, M. (2021). Power production of the hybrid Wavestar point absorber mounted around the Hywind spar platform and its dynamic response. Journal of Renewable and Sustainable Energy, vol. 13, no. 3.

[36] Ghafari, H. R., Ghassemi, H., & He, G. (2021). Numerical study of the Wavestar wave energy converter with multi-point-absorber around DeepCwind semisubmersible floating platform. Ocean Engineering, vol. 232, p. 109177. doi: 10.1016/J.OCEANENG.2021.109177.

[37] Ghafari, H. R., Ghassemi, H., & Neisi, A. (2022). Power matrix and dynamic response of the hybrid Wavestar-DeepCwind platform under different diameters and regular wave conditions. Ocean Engineering, vol. 247, p. 110734. doi: 10.1016/J.OCEANENG.2022.110734.

[38] Dorostkar, R., Abazari, A., & Ebrahimi, A. (2022). Energy harvesting through an integrated design of a semi-submersible offshore platform with point absorber wave energy converters. International Journal of Coastal, Offshore and Environmental Engineering, vol. 7, no. 4, pp. 27–36.

[39] Jokar, H., Abazari, A., & Dorostkar, R. (2024). Performance evaluation of a hybrid system of dhow ship and wave energy converter for power generation. Renewable Energy Research and Applications.

[40] Gharechae, A., Abazari, A., & Ketabdari, M. J. (2022). A semi-analytical solution for energy harvesting via the elastic motion of the circular floater of aquaculture cages attached with piezoelectric. Renewable Energy, vol. 196, pp. 181–194. doi: 10.1016/J.RENENE.2022.06.093.

[41] Gharechae, A., Abazari, A., & Soleimani, K. (2024). Performance assessment of a combined circular aquaculture cage floater and point absorber wave energy converters. Ocean Engineering, vol. 300, p. 117239. doi: 10.1016/J.OCEANENG.2024.117239.

[42] Cascajo, R., García, E., Quiles, E., Correcher, A. & Morant, F. (2019). Integration of marine wave energy converters into seaports: A case study in the port of Valencia. Energies, vol. 12, no. 5. doi: 10.3390/en12050787.

[43] Buccino, M., Stagonas, D. & Vicinanza, D. (2015). Development of a composite sea wall wave energy converter system. Renewable Energy, vol. 81. doi: 10.1016/j.renene.2015.03.010.

[44] Beharie, R. A. (2011). Measurements of shoreline wave action to establish possible environmental and ecological effects from wave energy converter arrays. EWTEC 2011 Proceedings, 2011.

[45] Copping, A. E., Hemery, L. G., Viehman, H., Seitz, A. C., Staines, G. J. & Hasselman, D. J. (2021). Are fish in danger? A review of environmental effects of marine renewable energy on fishes. Biological Conservation, vol. 262, p. 109297, Oct. doi: 10.1016/J.BIOCON.2021.109297.

[46] Akbarifard, S. & Radmanesh, F. (2018). Predicting sea wave height using Symbiotic Organisms Search (SOS) algorithm. Ocean Engineering, vol. 167. doi: 10.1016/j.oceaneng.2018.04.092.

[47] Roshan, G., Arab, M. & Klimenko, V. (2019). Modeling the impact of climate change on energy consumption and carbon dioxide emissions of buildings in Iran. Journal of Environmental Health Science & Engineering, vol. 17, no. 2, pp. 889–906. doi: 10.1007/s40201-019-00406-6.

[48] Afarin, M., Hamzeh, M. A. & Negarestan, H. (2015). Sedimentological and geomorphological classification of Chabahar coastal area (Chabahar-Gawater). Journal of Persian Gulf, vol. 6, no. 21, pp. 51–64. Available: http://jpg.inio.ac.ir/article-1-415-en.html. Accessed: Mar. 13, 2023.

[49] Darya Bandar Consulting Engineers. (2019). The executive package for acquiring electricity from solar energy: Economic and technical studies for the 1.2 MW power plant at the Shahid Beheshti Port (in Persian). Tehran.

[50] Aghaei, B., Arasteh, A. M., Lari, K. & Torabi Azad, M. (2021). Numerical modeling of wave reflection from sloped impermeable seawalls using the SPH method: Case study of Chabahar Port. Advances in Civil Engineering, vol. 2021. doi: 10.1155/2021/7382416.

[51] Defne, Z., Haas, K. A. & Fritz, H. M. (2009). Wave power potential along the Atlantic coast of the southeastern USA. Renewable Energy, vol. 34, no. 10. doi: 10.1016/j.renene.2009.02.019.

[52] Aydoğan, B., Ayat, B. & Yüksel, Y. (2013). Black Sea wave energy atlas from 13 years hindcasted wave data. Renewable Energy, vol. 57. doi: 10.1016/j.renene.2013.01.047.

[53] Ayat, B. (2013). Wave power atlas of Eastern Mediterranean and Aegean Seas. Energy, vol. 54. doi: 10.1016/j.energy.2013.02.060.

[54] Babarit, A., Hals, J., Muliawan, M. J., Kurniawan, A., Moan, T. & Krokstad, J. (2012). Numerical benchmarking study of a selection of wave energy converters. Renewable Energy, vol. 41. doi: 10.1016/j.renene.2011.10.002.

[55] Beels, C., et al. (2011). A methodology for production and cost assessment of a farm of wave energy converters. Renewable Energy, vol. 36, no. 12, pp. 3402–3416, Dec. doi: 10.1016/J.RENENE.2011.05.019.

[56] Eden, J. A. (2013). Optimum design of the Pelamis wave energy converter.

[57] Development of Marine Energy in New Zealand. (2008).

[58] Marquis, L., Kramer, M., Kringelum, J., Chozas, J. F. & Helstrup, N. E. (2012). Introduction of Wavestar wave energy converters at the Danish offshore wind power plant Horns Rev 2.

[59] Diaconu, S. & Rusu, E. (2013). Evaluation of various WEC devices in the Romanian near shore. WSEAS Conference, 2013.

[60] Guillou, N. & Chapalain, G. (2018). Annual and seasonal variabilities in the performances of wave energy converters. Energy, vol. 165. doi: 10.1016/j.energy.2018.10.001.

[61] Einali, A., Nemati, M. H., Banijamali, B. & Hoseini, H. (2022). Prioritize renewable energy resources in main Iranian ports area using AHP method. International Journal of Coastal, Offshore and Environmental Engineering, vol. 7, no. 4, pp. 7–16. doi: 10.22034/ijcoe.2022.166318.

[62] Leng, G. J. (1998). Renewable energy technologies project assessment tool, RETScreen. Energy Diversification Research Laboratory Canada, Varennes, Quebec.

[63] de Oliveira, L., dos Santos, I. F. S., Schmidt, N. L., Tiago Filho, G. L., Camacho, R. G. R. & Barros, R. M. (2021). Economic feasibility study of ocean wave electricity generation in Brazil. Renewable Energy, vol. 178. doi: 10.1016/j.renene.2021.07.009.